Int. J. Solids Structures, 1966, Vol. 2, pp. 591 to 603. Pergamon Press Ltd. Printed in Great Britain

LARGE DEFLECTIONS OF DIAMOND-SHAPED FRAMES*

J. A. JENKINS†, T. B. SEITZ‡ and J. S. PRZEMIENIECKI

Air Force Institute of Technology
Wright-Patterson Air Force Base, Ohio

Abstract—The nonlinear solutions for the large deflections of diamond-shaped frames are derived. The frames are loaded by forces applied at a pair of opposite joints, which are either pin-jointed or rigid. The experimental results obtained on square steel frames are compared with the nonlinear (exact) solutions and also with small deflection nonlinear and linear analyses. Stability of such frames under compressive loading is discussed and interpreted by both small and large deflection theories. The exact solutions are based on the assumption that the material is perfectly elastic and that the shear deformations are negligible. The deficiencies of the small deflection theories are made clear in this investigation.

NOTATION

E	Young's modulus
$E(k)$, $E(\bar{k})$	complete elliptic integrals of the second kind
$E(\theta, k)$, $E(\bar{\theta}, \bar{k})$	incomplete elliptic integrals of the second kind
$F(\theta, k)$, $F(\bar{\theta}, \bar{k})$	incomplete elliptic integrals of the first kind
$K(k)$, $K(\bar{k})$	complete elliptic integrals of the first kind
I	second moment of area
k^2	variable defined by equation (10)
$\bar{k}^2$	variable defined by equation (25)
l	member length
M	bending moment
M_0, $\overline{M}_0$	bending moment at the rigid end of member in pinned-fixed frame for tensile and compressive loading, respectively.
s	distance along the axis of member
u, $\bar{u}$	joint deflection relative to the rigid end in the direction normal to the tensile and compressive loads, respectively; positive directions defined in Fig. 1
v, $\bar{v}$	joint deflection relative to the rigid end in the direction of W and $\overline{W}$, respectively
$2W$, $2\overline{W}$	tensile and compressive loading on frame, respectively
w	normal deflection of member (small deflection theory)
x, y	Cartesian coordinates
η^2	Wl^2/EI, tensile load parameter
$\bar{\eta}^2$	$\overline{W}l^2/EI$, compressive load parameter
θ, $\bar{\theta}$	angles defined by equations (9) and (24)
ϕ	angle between the tangent to the deflected number at a point and the x axis
ϕ_0	angle at the rigid joint
ϕ_l	angle at the pinned joint

INTRODUCTION

NUMERICAL methods using finite element idealization are being currently developed for the nonlinear analysis of structures made up from beams with either pin-jointed or rigid

* This paper is based on a thesis by the first two authors submitted in partial fulfillment of the requirement for the degree of Master of Science at the Air Force Institute of Technology.

† Now with: Air Force Systems Command, L.G. Hanscom Field, Massachusetts.

‡ Now with: Air Force Systems Command, Vandenberg AFB, California.

connections. In order to check accuracy of these methods exact solutions are required for large deflections and the analysis of diamond-shaped frames has been selected for this purpose.

Studies of large deflections, which require nonlinear solutions, have been concerned mainly with single members. Large deflections in cantilever beams subjected to concentrated and uniformly distributed loads were studied by Barten [1], Bisshopp and Drucker [2], Rohde [3], and Scott and Carver [4]. Simply supported beams were analyzed by Conway [5], Scott and Carver [4], and Gospodnetic [6], while Wang *et al.* [7] developed numerical analysis for beams carrying arbitrary loading. Recently Kerr [8] developed an exact analysis for large deflections in a square frame with rigid corners loaded at the midpoints of a pair of opposite sides. The structure analyzed in this paper is a diamond-shaped frame subjected to either tensile or compressive loading applied at a pair of opposite joints. The loaded joints can be either pinned or rigid.

The analysis of the frame deflections presented in this paper may be regarded as an extension of the beam-column solution to large deflections. The method of solution used is similar to that of the elastica discussed by Timoshenko and Gere [9]. The solution for deflections is obtained in terms of elliptic integrals and a computer program has been written to compute not only deflections of the joints but also the deformed shapes of the frame. Experimental data obtained on square frames agreed very closely with the large deflection theoretical results. In addition, small deflection nonlinear and linear analyses were used for comparison with the experimental data.

LARGE DEFLECTION ANALYSIS: PINNED-FIXED FRAME

(*a*) *Tensile loading*

The frame geometry and loading are shown in Fig. 1(a). Because of symmetry of the frame it is sufficient to analyze only one frame member. The equilibrium equations for large deflections must be based on the deformed configuration as shown in Fig. 1 so that the Euler–Bernoulli equation for bending due to tensile loading must be expressed as

$$\frac{d\phi}{ds} = \frac{M}{EI} = \frac{W}{EI}(l\cos\phi_0 - u - x). \tag{1}$$

Differentiating equation (1) with respect to s and introducing a nondimensional load parameter $\eta^2 = Wl^2/EI$ we obtain

$$\frac{d^2\phi}{ds^2} = -\frac{W}{EI}\frac{dx}{ds} = \frac{-\eta^2}{l^2}\cos\phi. \tag{2}$$

Integrating equation (2)

$$\left(\frac{d\phi}{ds}\right)^2 = -\frac{2\eta^2}{l^2}\sin\phi + C \tag{3}$$

where the constant C may be determined from the boundary condition

$$\frac{d\phi}{ds} = 0 \quad \text{at} \quad \phi = \phi_l. \tag{4}$$

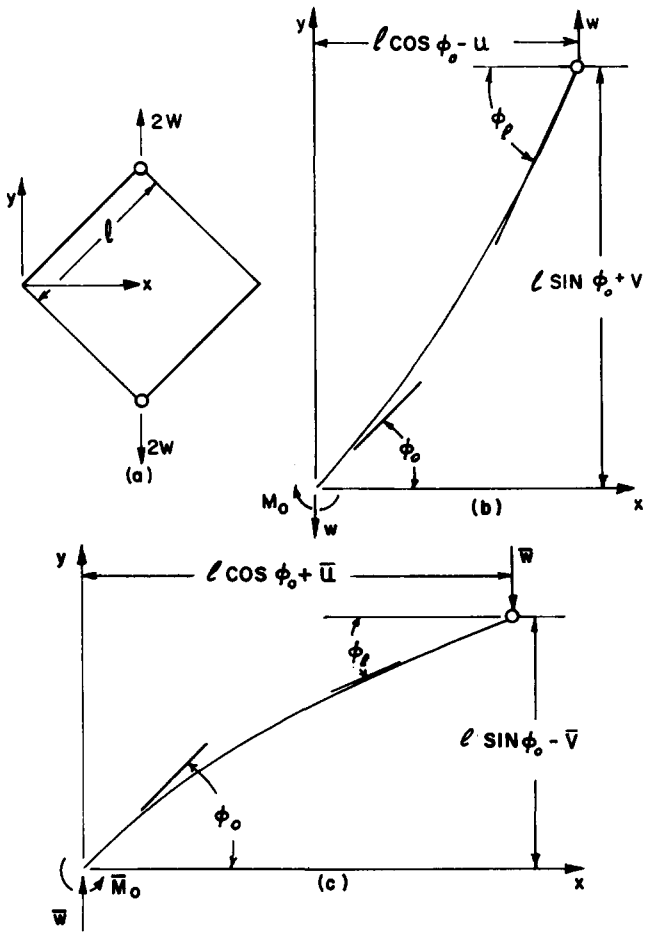

FIG. 1. Pinned-fixed frame: (a) undeformed frame, (b) large deflections in tension, (c) large deflections in compression.

Hence

$$\pm\frac{d\phi}{ds} = \frac{\eta}{l}\sqrt{[2(\sin\phi_l - \sin\phi)]}. \tag{5}$$

Now for small values of s the value of $d\phi/ds$ is positive and $\sin\phi_l > \sin\phi$; consequently, the positive sign must be taken in the ambiguity on the left of equation (5).

Observing that

$$\frac{d\phi}{ds} = \frac{d\phi}{dy}\frac{dy}{ds} = \frac{d\phi}{dy}\sin\phi \tag{6}$$

the projection of the deformed member on the y axis may be calculated from

$$l\sin\phi_0 + v = \int_0^{l\sin\phi_0 + v} dy \tag{7}$$

Using equations (5), (6) and (7) we have

$$\eta\left(\sin\phi_0+\frac{v}{l}\right)=\int_{\phi_0}^{\phi_l}\frac{\sin\phi\,\mathrm{d}\phi}{\sqrt{[2(\sin\phi_l-\sin\phi)]}}. \tag{8}$$

Introducing now a new variable θ such that

$$\sin^2\theta=(1+\sin\phi)/2k^2 \tag{9}$$

where

$$2k^2=1+\sin\phi_l \tag{10}$$

equation (8) may be transformed into

$$\eta\left(\sin\phi_0+\frac{v}{l}\right)=\int_{\theta_1}^{\theta_2}\frac{(2k^2\sin^2\theta-1)}{\sqrt{[1-k^2\sin^2\theta]}}\mathrm{d}\theta \tag{11}$$

where

$$\sin^2\theta_1=(1+\sin\phi_0)/(1+\sin\phi_l) \tag{12}$$

and

$$\theta_2=\pi/2. \tag{13}$$

The integral on the right of equation (11) is expressible in terms of elliptic integrals and it can be shown that

$$\eta\left(\sin\phi_0+\frac{v}{l}\right)=K(k)-F(\theta_1,k)-2E(k)+2E(\theta_1,k) \tag{14}$$

where $K(k)$ and $F(\theta_1, k)$ are, respectively, complete and incomplete elliptic integrals of the first kind with modulus k, while $E(k)$ and $E(\theta_1, k)$ are, respectively, complete and incomplete elliptic integrals of the second kind.

Similarly to develop an expression for the projection of the deformed member on the x axis we use

$$\frac{\mathrm{d}\phi}{\mathrm{d}s}=\frac{\mathrm{d}\phi}{\mathrm{d}x}\,\frac{\mathrm{d}x}{\mathrm{d}s}=\frac{\mathrm{d}\phi}{\mathrm{d}x}\cos\phi \tag{15}$$

and

$$l\cos\phi_0-u=\int_0^{l\cos\phi_0-u}\mathrm{d}x. \tag{16}$$

From equations (15) and (16) it follows that

$$\eta\left(\cos\phi_0-\frac{u}{l}\right)=\int_{\phi_0}^{\phi_l}\frac{\cos\phi\,\mathrm{d}\phi}{\sqrt{[2(\sin\phi_l-\sin\phi)]}}. \tag{17}$$

Using again the variable θ, defined by equation (5), we obtain from equation (17)

$$\eta\left(\cos\phi_0-\frac{u}{l}\right)=\int_{\theta_1}^{\theta_2}2k\sin\theta\,\mathrm{d}\theta=2k\cos\theta_1. \tag{18}$$

In equations (14) and (18) ϕ_l appears as an unknown angle and thus an additional relationship is required in order to solve for the deflections u and v. This relationship is obtained from the condition of inextensibility of the member, i.e.

$$l = \int_0^l \mathrm{d}s = \frac{l}{\eta}\int_{\phi_0}^{\phi_l} \frac{\mathrm{d}\phi}{\sqrt{[2(\sin\phi_l - \sin\phi)]}} \tag{19}$$

which may be transformed, using equations (9), (10), (12) and (13), into

$$\eta = \int_{\theta_1}^{\theta_2} \frac{\mathrm{d}\theta}{\sqrt{[1-k^2\sin^2\theta]}} = K(k) - F(\theta_1, k). \tag{20}$$

The derivation of equations for the deflected shape of the member is similar to that for the deflection of the end points of the member, except that the integrations involved must be carried out over the interval ϕ_0 to ϕ instead of ϕ_0 to ϕ_l. Replacing θ_2 by θ in equations (11) and (18) and noting that the projected lengths are simply y and x, respectively, we obtain

$$\eta y/l = F(\theta, k) - F(\theta_1, k) - 2E(\theta, k) + 2E(\theta_1, k) \tag{21}$$

and

$$\eta x/l = 2k(\cos\theta_1 - \cos\theta). \tag{22}$$

Solutions to equations (20), (21) and (22) have been obtained on an IBM 7094 computer using subroutines for elliptic integrals. Some deformed shapes for a square frame are shown in Fig. 2 for several values of the loading parameter η^2.

(*b*) *Compressive loading*

The basic equation for bending of the member under compressive loading, as shown in Fig. 1(c), is given by

$$\frac{\mathrm{d}\phi}{\mathrm{d}s} = -\frac{\overline{W}}{EI}(l\cos\phi_0 + \bar{u} - x). \tag{23}$$

Following a procedure analogous to that for the case of tensile loading and employing a new variable $\bar{\theta}$ such that

$$\sin^2\bar{\theta} = (1-\sin\phi)/2\bar{k}^2 \tag{24}$$

where

$$2\bar{k}^2 = 1 - \sin\phi_l \tag{25}$$

we obtain the following equations:

$$\bar{\eta}\left(\sin\phi_0 - \frac{\bar{v}}{l}\right) = K(\bar{k}) - F(\bar{\theta}_1, \bar{k}) - 2E(\bar{k}) + 2E(\bar{\theta}_1, \bar{k}) \tag{26}$$

$$\bar{\eta}\left(\cos\phi_0 + \frac{\bar{u}}{l}\right) = -2\bar{k}\cos\bar{\theta}_1 \tag{27}$$

$$\bar{\eta} = F(\bar{\theta}_1, \bar{k}) - K(\bar{k}) \tag{28}$$

$$\bar{\eta}y/l = F(\bar{\theta}, \bar{k}) - F(\bar{\theta}_1, \bar{k}) - 2E(\bar{\theta}, \bar{k}) + 2E(\bar{\theta}_1, \bar{k}) \tag{29}$$

$$\bar{\eta}x/l = 2\bar{k}(\cos\bar{\theta} - \cos\bar{\theta}_1) \tag{30}$$

where

$$\sin^2\bar{\theta}_1 = (1 - \sin\phi_0)/(1 - \sin\phi_l) \tag{31}$$

and

$$\bar{\eta}^2 = \overline{W}l/EI. \tag{32}$$

It should be noted from the sign convention used in Fig. 1 that $\bar{\eta}^2 = -\eta^2$ and that the positive signs of $\bar{u}$ and $\bar{v}$ are opposite to those of u and v.

Typical deformed shapes for a square frame are shown in Fig. 2 for $\eta^2 = -1$ and -12. Variation of the elongation or contraction of the frame diagonals with the applied loading is plotted in Figs. 3 and 4. These plots and the deformed frame shapes have been obtained from the computer solutions of the equations for the joint deflections and the x and y coordinates. The asymptotic values of deflections shown in Figs. 3 and 4 may be predicted from the frame geometry. When the applied compressive loading is sufficiently high the opposite members of the frame will theoretically pass through each other as shown by the deformed shape for $\eta^2 = -12$ in Fig. 2. This is also accompanied by the reversal of slope of the load–horizontal elongation curve as illustrated in Fig. 4.

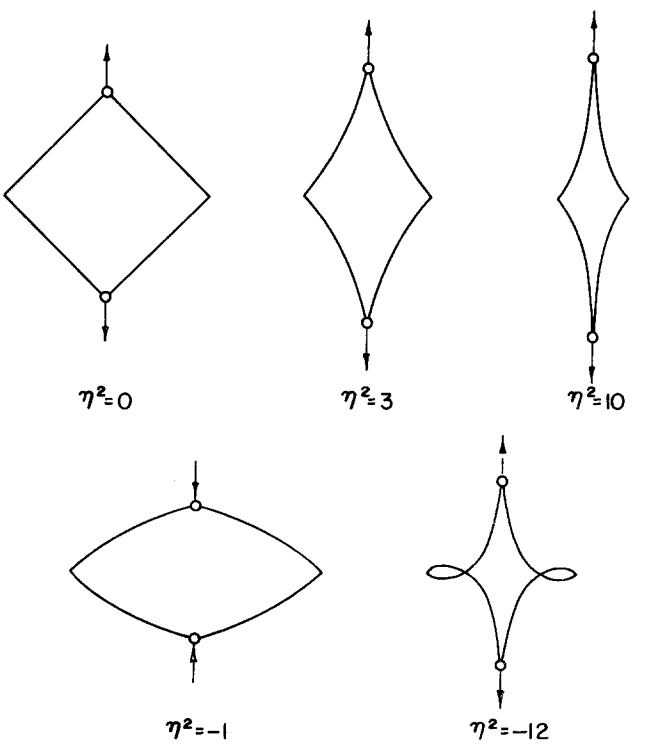

FIG. 2. Deformed shapes of a square pinned-fixed frame for different values of the loading parameter η^2.

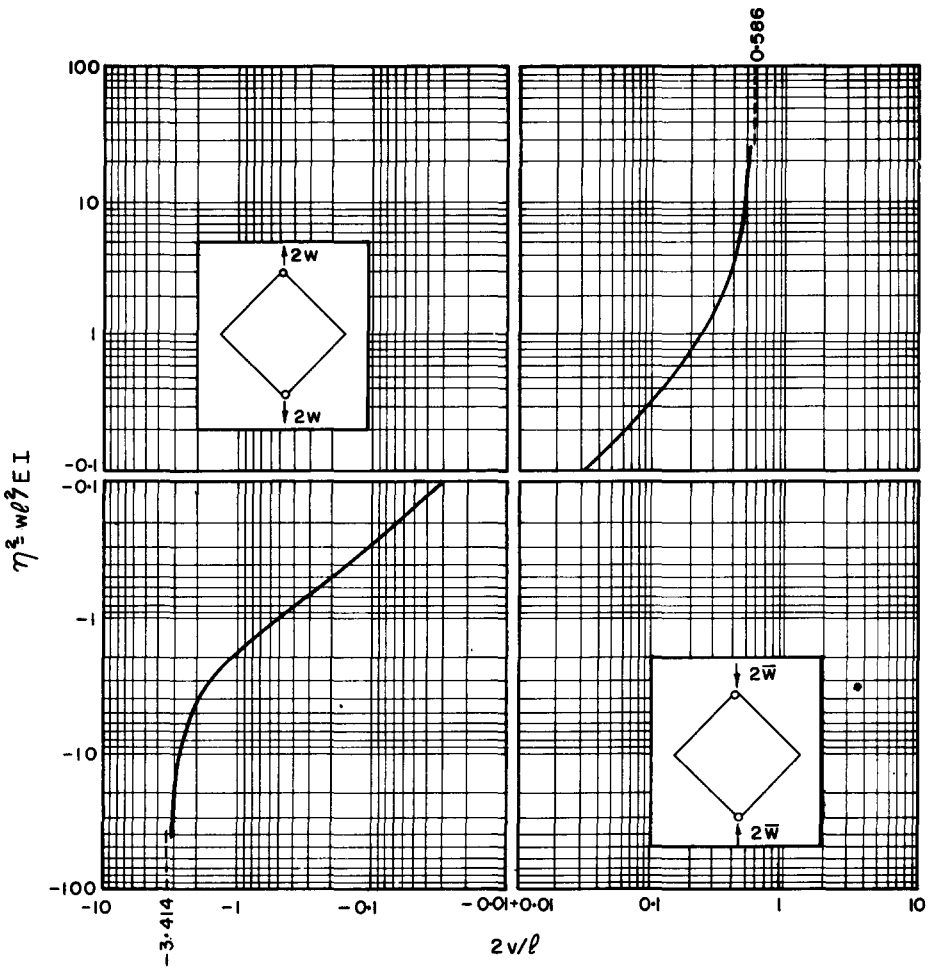

FIG. 3. Vertical elongation (or contraction) of a square pinned-fixed frame.

LARGE DEFLECTION ANALYSIS: FIXED-FIXED FRAME

The frame geometry is shown in Figs. 5(a) and 5(b). Because of symmetry of the frame, points of inflection on each member are located midway between its ends. Since at the point of inflection the bending moment is zero it follows that the solution for deflections of the fixed-fixed frame can be derived from the previous solution for the pinned-fixed frame.

Typical deformed shapes for a square, fixed-fixed frame are shown in Fig. 6 for several different values of the loading parameter η^2.

SMALL DEFLECTION ANALYSIS

(*a*) *Pinned-fixed frame*

For small deflections $d\phi/ds \approx d^2w/ds^2$ where w is the deflection normal to the frame member. The Euler–Bernoulli equation for the deflection w can be solved explicitly and

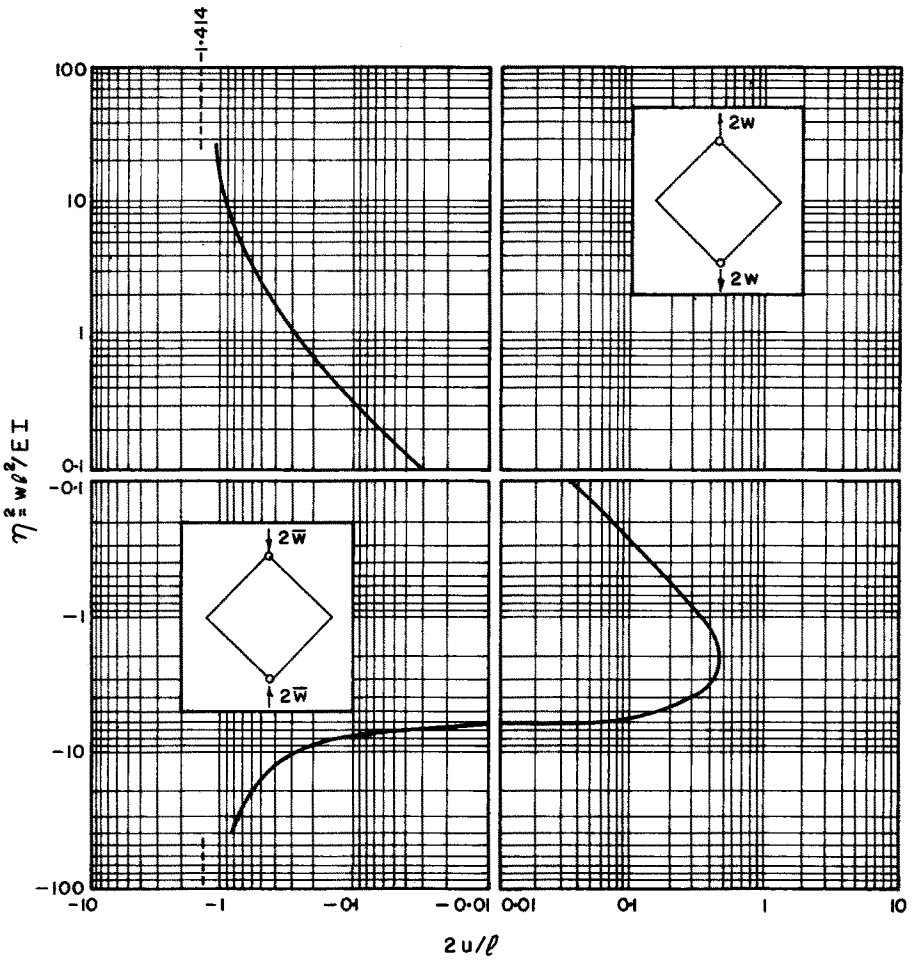

FIG. 4. Horizontal contraction (or elongation) of a square pinned-fixed frame.

then noting that the tangential deflection (along the member) must be equal to zero we can resolve w into u and v components. Subsequent analysis will be restricted to square frames which will be used for comparison with the exact theory. It can be demonstrated easily that for a square frame under tensile loading the joint deflections are given by

$$\frac{u}{l} = \frac{v}{l} = \frac{1}{2^{\frac{1}{2}}}\left[1 - \frac{2^{\frac{1}{2}}}{\eta}\tanh(\eta/2^{\frac{1}{2}})\right]. \tag{33}$$

Similarly for compressive loading

$$\frac{\bar{u}}{l} = \frac{\bar{v}}{l} = \frac{1}{2^{\frac{1}{2}}}\left[1 - \frac{2^{\frac{1}{2}}}{\bar{\eta}}\tan(\bar{\eta}/2^{\frac{1}{2}})\right]. \tag{34}$$

For infinitesimal deflections (linear theory) the right sides of equations (33) and (34) reduce to $Wl^2/6EI$ and $\overline{W}l^2/6EI$, respectively.

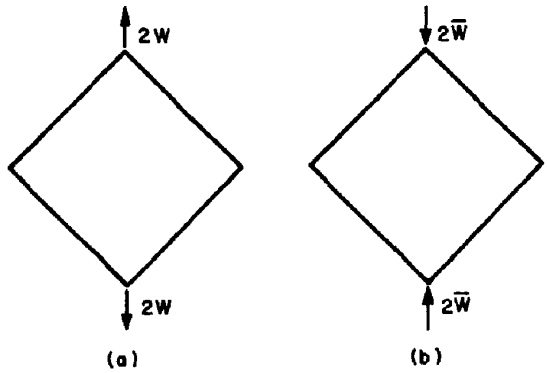

FIG. 5. Fixed-fixed frame.

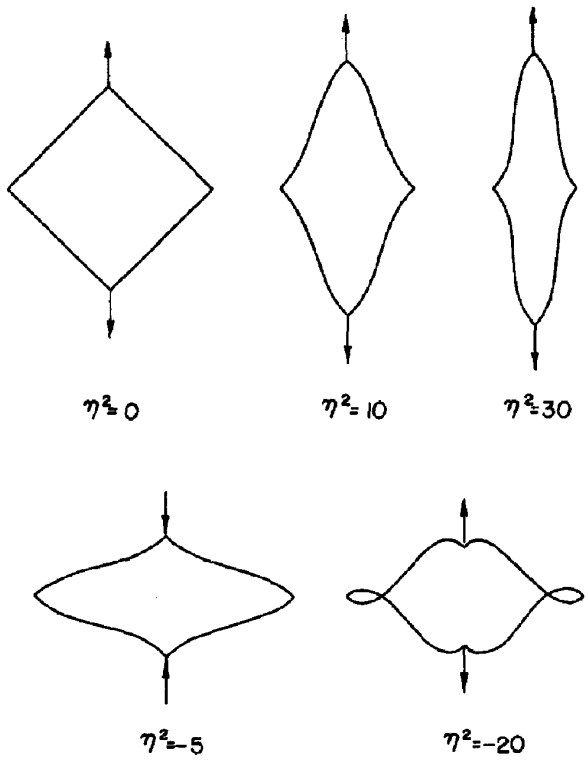

FIG. 6. Deformed shapes of a square fixed-fixed frame for different values of the loading parameter η^2.

(*b*) *Fixed-fixed frame*

For a square fixed-fixed frame under tensile loading

$$\frac{u}{l} = \frac{v}{l} = \frac{1}{2^{\frac{1}{2}}}\left[1 - \frac{2^{\frac{1}{2}}}{\eta}\tanh(\eta/2^{\frac{1}{2}})\right] \tag{35}$$

while for compressive loading

$$\frac{\bar{u}}{l} = \frac{\bar{v}}{l} = \frac{1}{2^{\frac{1}{4}}}\left[1 - \frac{2^{\frac{1}{4}}}{\bar{\eta}}\tan(\bar{\eta}/2^{\frac{1}{4}})\right]. \tag{36}$$

For infinitesimal deflections (linear theory) the right sides of equations (35) and (36) become $Wl^2/24EI$ and $\overline{W}l^2/24EI$, respectively.

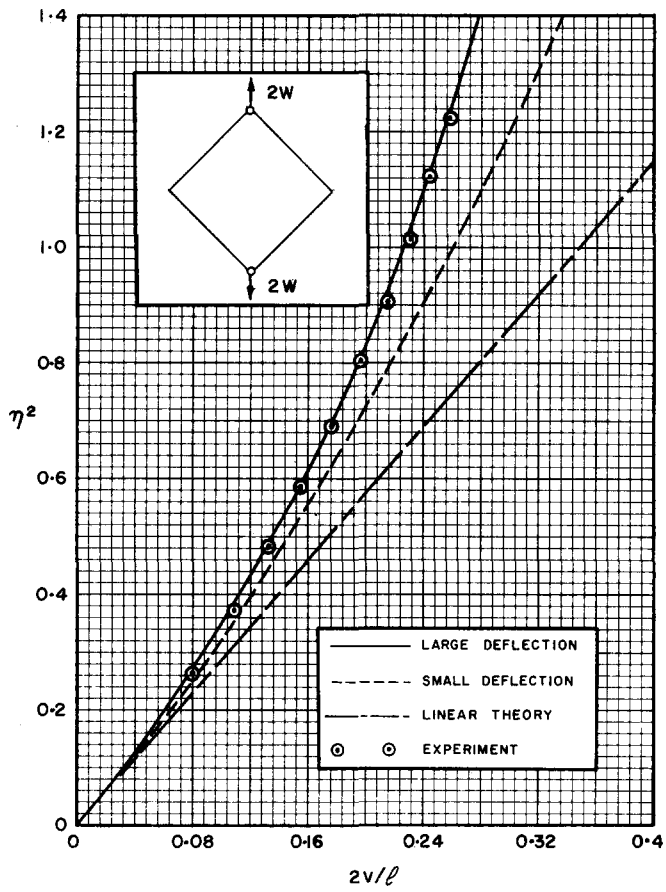

FIG. 9. Vertical elongation of pinned-fixed frame under tensile loading.

(*c*) *Stability*

The deflections predicted by the small deflection theory tend to infinity when the Euler buckling load is reached in the frame members. Perusal of equations (34) and (36) indicates that this occurs when $(\bar{\eta}/2^{\frac{1}{4}}) = \pi/2$ for pinned-fixed frame and when $(\bar{\eta}/2^{\frac{1}{4}}) = \pi/2$ for fixed-fixed frame. The exact theory, on the other hand, predicts a stable system, i.e. one in which deflections in the direction of the applied load are always increasing. This is demonstrated for the case of pinned-fixed frames in Fig. 3.

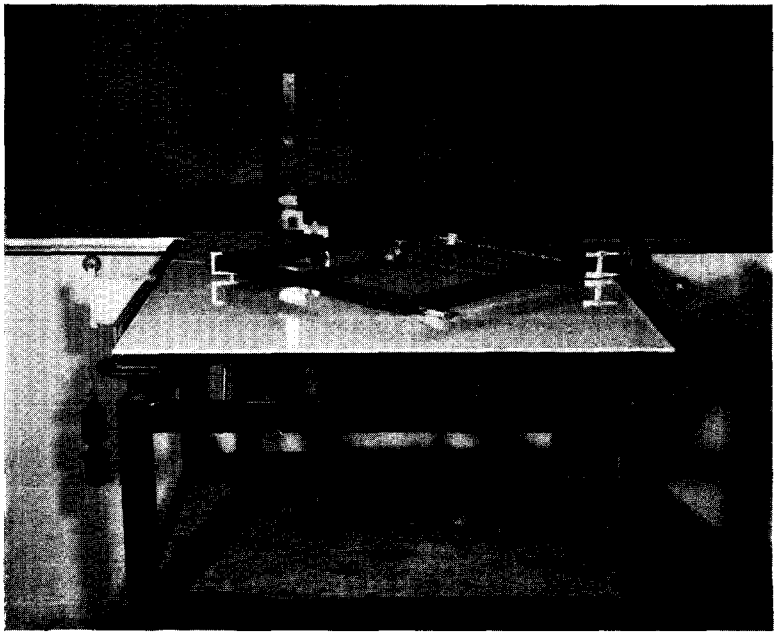

FIG. 7. Pinned-fixed frame loaded in tension.

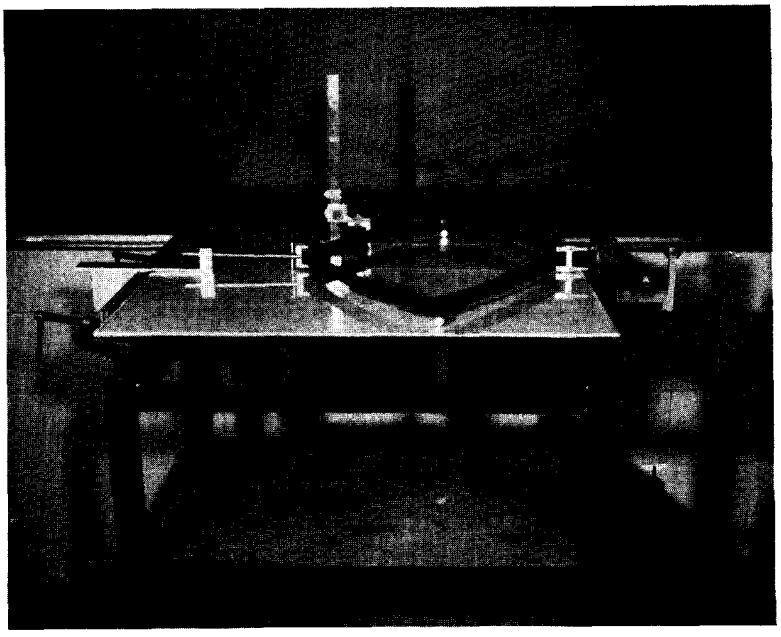

FIG. 8. Pinned-fixed frame loaded in compression.

[*facing page* 600

EXPERIMENTAL RESULTS AND CONCLUSIONS

Deflections predicted by the large deflection theory have been verified experimentally on square frames made from 4130 cold-rolled steel strip having $E = 28{\cdot}95 \times 10^6$ lb/in^2. Each member was 17 in. long of cross-section $1{\cdot}0 \times 0{\cdot}0625$ in. All fixed joints were constructed by welding the connecting members together over a special jig. The pinned joints were constructed by welding 1-in. steel hinges to the pinned members.

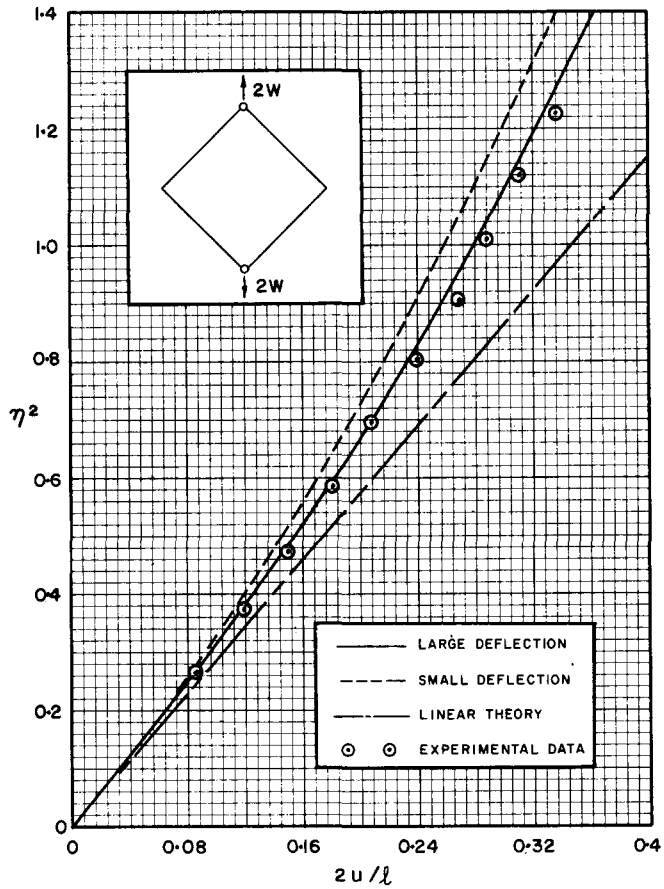

FIG. 10. Horizontal contraction of pinned-fixed frame under tensile loading.

The experimental set-up is shown in Figs. 7 and 8. Loading was applied by hanging dead weights from a system of cables attached to the frame. Deflections were read directly off a sheet of standard grid paper underneath a layer of plate glass over which the frames were positioned.

A comparison of the results of the various theories as well as an indication of the accuracy of the theoretical predictions of the large deflection analysis may be seen in Figs. 9, 10, 11 and 12. The large deflection theory gives results which are in excellent

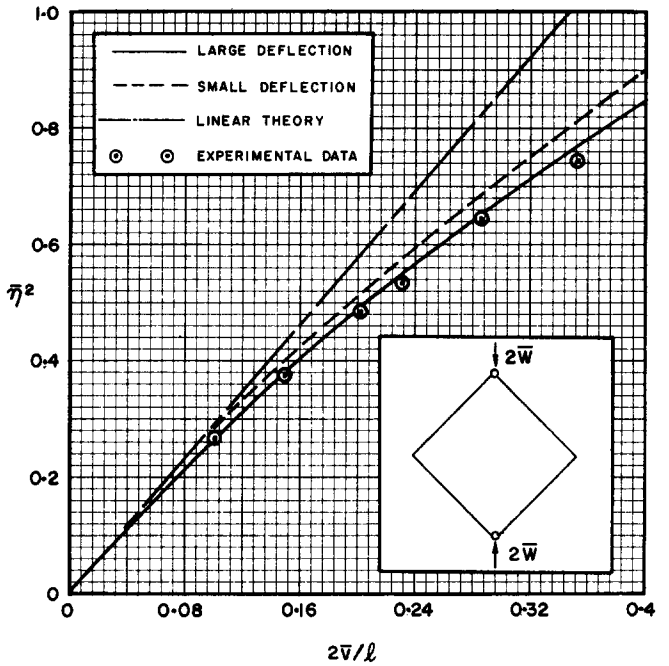

FIG. 11. Vertical contraction of pinned-fixed frame under compressive loading.

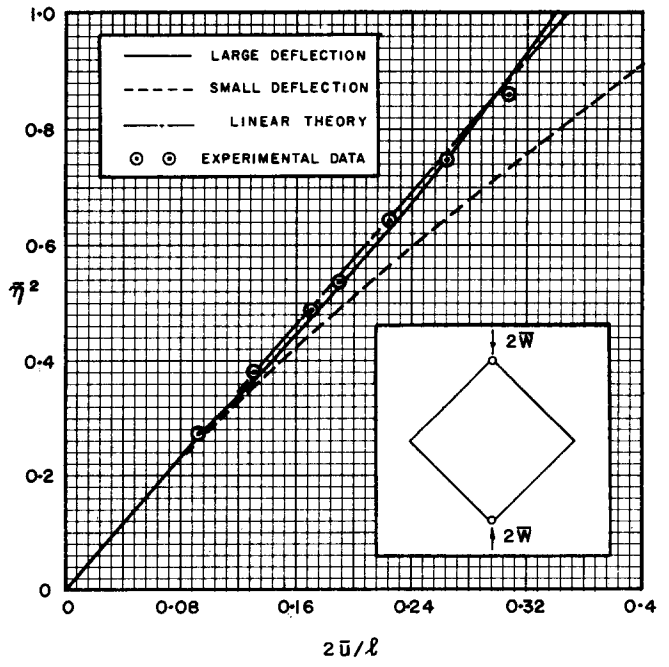

FIG. 12. Horizontal elongation of pinned-fixed frame under compressive loading.

agreement with the experimental measurements of deflections. It can be seen that for the range of deflections considered the small deflection nonlinear and linear analyses are unsatisfactory for predicting frame deflections and the large deflection analysis must be used.

REFERENCES

[1] H. J. BARTEN, On the deflection of a cantilever beam. *Q. appl. Math.* **2**, 168 (1944) and **3**, 275 (1945).
[2] K. E. BISSHOPP and D. C. DRUCKER, Large deflection of cantilever beams. *Q. appl. Math.* **3**, 272 (1945).
[3] F. V. ROHDE, Large deflections of a cantilever beam with uniformly distributed load. *Q. appl. Math.* **11**, 337 (1953).
[4] E. J. SCOTT and D. R. CARVER, On the nonlinear differential equation for beam deflection. *J. appl. Mech., Trans. ASME* **77**, 245 (1955).
[5] H. D. CONWAY, The large deflection of simply supported beams. *Phil. Mag.* **38**, 905 (1947).
[6] D. GOSPODNETIC, Deflection curve of a simply supported beam. *J. appl. Mech.* **26**, 675 (1959).
[7] T. M. WANG, S. L. LEE and O. C. ZIENKIEWICZ, A numerical analysis of large deflections of beams. *Int. J. mech. Sci.* **3**, 219 (1961).
[8] C. N. KERR, Large deflections of a square frame. *Q. Jl Mech. appl. Math.* **17**, 24 (1964).
[9] S. P. TIMOSHENKO and J. M. GERE, *Theory of Elastic Stability*, 2nd edition, pp. 76–82. McGraw-Hill (1961).

(*Received* 11 *October* 1965; *revised* 7 *February* 1966)

Résumé—Les solutions non-linéaires pour les grandes déviations de cadre losangique sont dérivées. Les cadres sont chargés de forces appliquées sur une paire de joints opposés, qui sont soit assemblés par des boulons, soit rigides. Les résultats expérimentaux obtenus sur des cadres d'acier carrés sont comparés avec la solution non-linéaire (exacte) ainsi qu'avec des analyses de légère déviation non-linéaire et linéaire. La stabilité de ces cadres sous des charges compressives est discutée et interprétée par des théories de grande et petite déviation. Les solutions exactes sont basées sur l'assomption que le materiel est de préférence élastique et que les déformations de cisaillement sont négligeables. Les déficiences des théories de petites déviations sont clairement démontrées dans cette investigation.

Zusammenfassung—Die nichtlinearen Lösungen für die grossen Abweichungen von rautenförmigen Rahmen sind abgeleitet. Die Rahmen sind von Kräften beansprucht welche in einem Paar von gegenüberliegenden Verbindungen angebracht sind, welche entweder bolzenverbunden oder starr sind. Die Versuchsergebnisse, erhalten an viereckigen Stahlgestellen, sind mit den nichtlinearen (exakten) Lösungen und auch mit kleinen Abweichungen von nichtlinearen und linearen Analysen verglichen. Die Stabilität von solchen Rahmen unter Durchbeladung ist erörtert und erklärt mit den beiden kleinen und grossen Abweichungstheorien. Die exakten Lösungen sind auf der Annahme begründet, dass das Material vollkommen elastisch ist und dass die Scherverformungen geringfügig sind. Die Unzulänglichkeiten der kleinen Abweichungstheorien sind in dieser Untersuchung klargestellt.

Абстракт—Выведены нелинейные решения для больших отклонений ромбовидных ферм. Фермы нагружены силами, приложенными у пары противоположных соединений, которые представляют из себя или шарнирные или жёсткие соединения. Экспериментальные результаты, полученные на квадратных стальных фермах сравниваются с нелинейными (точными) решениями и также с нелинейными и линейными анализами малого отклонения. Устойчивость таких ферм под сжимающей нагрузкой обсуждается и объясняется обеими теориями—теорией малого отклонения и теорией большого отклонения. Точные решения основаны на предположении, что мтаериал совершенно упруг и, что деформации сдвига—незначительны. В этом исследовании выясняются недостатки теорий малого отклонения.